

Physical Limitation of Phytoplankton Dynamics in Coastal Waters

Niu, Lixia; Van Gelder, P. H.A.J.M.; Vrijling, J. K.

DOI

[10.2112/JCOASTRES-D-15-00136.1](https://doi.org/10.2112/JCOASTRES-D-15-00136.1)

Publication date

2017

Document Version

Final published version

Published in

Journal of Coastal Research: an international forum for the Littoral Sciences

Citation (APA)

Niu, L., Van Gelder, P. H. A. J. M., & Vrijling, J. K. (2017). Physical Limitation of Phytoplankton Dynamics in Coastal Waters. *Journal of Coastal Research: an international forum for the Littoral Sciences*, 33(1), 88-95. <https://doi.org/10.2112/JCOASTRES-D-15-00136.1>

Important note

To cite this publication, please use the final published version (if applicable). Please check the document version above.

Copyright

Other than for strictly personal use, it is not permitted to download, forward or distribute the text or part of it, without the consent of the author(s) and/or copyright holder(s), unless the work is under an open content license such as Creative Commons.

Takedown policy

Please contact us and provide details if you believe this document breaches copyrights. We will remove access to the work immediately and investigate your claim.

Physical Limitation of Phytoplankton Dynamics in Coastal Waters

Authors: Niu, Lixia, van Gelder, P.H.A.J.M., and Vrijling, J.K.

Source: Journal of Coastal Research, 33(1) : 88-95

Published By: Coastal Education and Research Foundation

URL: <https://doi.org/10.2112/JCOASTRES-D-15-00136.1>

BioOne Complete (complete.BioOne.org) is a full-text database of 200 subscribed and open-access titles in the biological, ecological, and environmental sciences published by nonprofit societies, associations, museums, institutions, and presses.

Your use of this PDF, the BioOne Complete website, and all posted and associated content indicates your acceptance of BioOne's Terms of Use, available at www.bioone.org/terms-of-use.

Usage of BioOne Complete content is strictly limited to personal, educational, and non - commercial use. Commercial inquiries or rights and permissions requests should be directed to the individual publisher as copyright holder.

BioOne sees sustainable scholarly publishing as an inherently collaborative enterprise connecting authors, nonprofit publishers, academic institutions, research libraries, and research funders in the common goal of maximizing access to critical research.

Physical Limitation of Phytoplankton Dynamics in Coastal Waters

Lixia Niu^{†*}, P.H.A.J.M. van Gelder[‡], and J.K. Vrijling[†]

[†]Department of Hydraulic Engineering
Delft University of Technology
Delft 2628 CN, The Netherlands

[‡]Section of Safety and Security Science
Delft University of Technology
Delft 2628 BX, The Netherlands



www.cerf-jcr.org



www.JCRonline.org

ABSTRACT

Niu, L.; van Gelder, P.H.A.J.M., and Vrijling, J.K., 2017. Physical limitation of phytoplankton dynamics in coastal waters. *Journal of Coastal Research*, 33(1), 88–95. Coconut Creek (Florida), ISSN 0749-0208.

Research on phytoplankton dynamics in coastal waters has frequently been proposed, motivated by environmental factors. The present study aims to develop a vertical phytoplankton model to investigate the phytoplankton variability in a case of the Jiangsu coastal waters, driven by physical limitation. The quality of the parameter estimation largely determines the reliability of the model output. Skill assessment results reveal that the vertical phytoplankton model is able to reproduce reliable predictions of phytoplankton biomass in this case. Significant correlations are established between phytoplankton biomass and chlorophyll *a*. The phytoplankton biomass is significantly correlated with the variables of temperature, light attenuation coefficient, and euphotic depth. A decrease of phytoplankton biomass corresponds to deeper water, excluding the case of Yangkou station. Particular attention has been paid to the depth-averaged phytoplankton biomass. In the presence of uncertainty, the bootstrap method is used to derive a 95% confidence interval of the estimate, as well as mean value, standard deviation, and skewness. The findings of this study contribute to understanding of the coastal ecosystem and coastal management.

ADDITIONAL INDEX WORDS: *Phytoplankton variability, coastal ecosystem.*

INTRODUCTION

There is increasing concern about the role of phytoplankton and its effect on coastal ecosystems. The investigation of phytoplankton dynamics (*i.e.* growth, loss, biomass, and bloom) has provided insights into the coastal ecosystem (Cloern, 1996; Cloern, Foster, and Kleckner, 2014; Edolvang *et al.*, 2005; Fu *et al.*, 2009; Godrijan *et al.*, 2013; Pedersen and Borum, 1996). Phytoplankton has been explained as a consequence of environmental variables. Temperature and light intensity are closely related to the growth of phytoplankton (Eppley, 1972; Geider, MacIntyre, and Kana, 1998; Ormofsdottir, Lumsden, and Pinckney, 2004). A change of salinity has an effect on the phytoplankton community (Lionard *et al.*, 2005; Schmidt, 1999). Wind stress and tidal currents affect the turbulent mixing rate, determining the vertical distributions of phytoplankton biomass (Serra *et al.*, 2007; Woernle, Dijkstra, and van der Woerd, 2014; Wong, Lee, and Hodgkiss, 2007) and affecting the species composition because of the effects on the availability of light intensity and nutrients (Ferris and Christian, 1991). Suspended sediment absorbs and scatters light intensity, implying that phytoplankton is limited by light availability in the high turbidity zone (Wild-Allen, Lane, and Tett, 2002). Among all the environmental factors, phytoplankton dynamics is mainly refined by the limitations of light and nutrient availability (Boyer *et al.*, 2009; Cloern, 1987; Eilers and Peeters, 1988).

In the context of limited observations, mathematical models are convenient and flexible for investigating phytoplankton dynamics (Evans and Parslow, 1985; Franks, 1997, 2002; Murray and Parslow, 1999; Riley, Stommel, and Bumpus, 1949). From the physical properties, studies of phytoplankton dynamics have been proposed in several cases (Sharples, 2007; Sharples *et al.*, 2001; Williams and Rhines, 2010). The case study area of the Jiangsu coastal zone is bounded by Shandong Peninsula and connected to the Yellow Sea, shown in Figure 1. In this study, a vertical phytoplankton model is developed to investigate phytoplankton variability from the physical limitation. With respect to uncertainty, the bootstrap method is introduced to give insight into the predictions with a characterization of uncertainty analysis.

METHODS

The samples used in this study are derived from two sources: (1) National Aeronautics and Space Administration (NASA) monitoring data (NASA, 2015) processed with SeaDAS 7.0, including chlorophyll *a* (*Chla*, in milligrams per cubic meter), phytoplankton biomass (*P*, in grams per cubic meter), light attenuation coefficient (K_d , in reciprocal days), light intensity (*I*, Einstein in reciprocal square meters per day), euphotic depth (Z_e , in meters), and ambient water temperature (*T*, in degrees Celsius), and (2) field observations provided by the Hydrological Bureau of the Yangtze Water Conservancy Committee, including water depth, velocity, salinity, suspended sediment, and wind profiles.

Phytoplankton Model

In the general form, the characteristics of phytoplankton dynamics are coupled with a physical model (advection–diffusion equation), written as

DOI: 10.2112/JCOASTRES-D-15-00136.1 received 24 June 2015; accepted in revision 1 November 2015; corrected proofs received 4 December 2015; published pre-print online 30 December 2015.

*Corresponding author: xiaoxia3623@gmail.com

©Coastal Education and Research Foundation, Inc. 2017

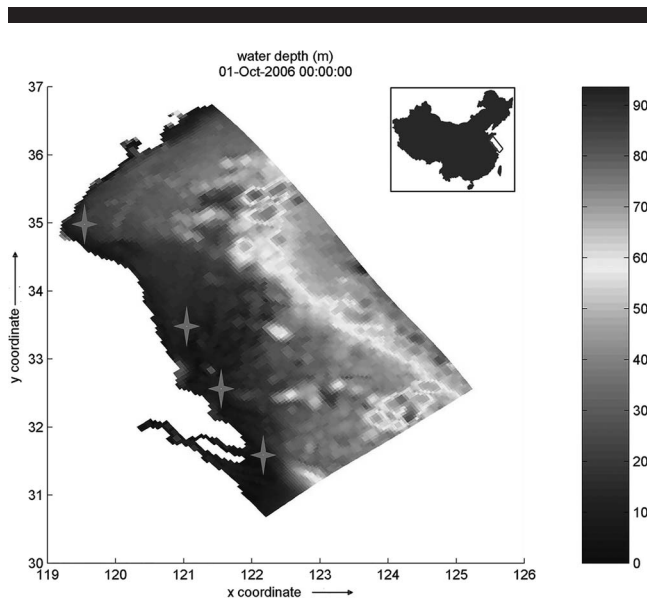


Figure 1. Case location and bathymetry of the Jiangsu coastal zone (from north to south, stars indicate Lianyungang station, Dafeng station, Yangkou station, and the north branch of the Yangtze River estuary).

$$\begin{aligned} \frac{\partial C}{\partial t} + u_x \frac{\partial C}{\partial x} + u_y \frac{\partial C}{\partial y} + (u_z + u_s) \frac{\partial C}{\partial z} \\ = E_h \left(\frac{\partial^2 C}{\partial x^2} + \frac{\partial^2 C}{\partial y^2} \right) + E_z \frac{\partial^2 C}{\partial z^2} + \text{phytoplankton dynamics} \end{aligned} \quad (1)$$

where C denotes the concentration of the state variable, expressed in grams per cubic meter; u_x , u_y , and u_z denote the velocities in the x , y , and z directions, expressed in meters per second; E_h and E_z denote the horizontal and vertical turbulent diffusivity, expressed in square meters per second; and u_s denotes the sinking velocity, expressed in meters per second.

Phytoplankton dynamics is described in the form of

$$\begin{aligned} \frac{dP}{dt} &= \mu \times P - g \times Z - l \times P \\ \frac{dZ}{dt} &= \gamma g \times Z - l' \times Z \end{aligned} \quad (2)$$

where Z denotes zooplankton biomass, expressed in grams per cubic meter; μ denotes specific growth rate, expressed in reciprocal days; l denotes loss rate by mortality, respiration, and metabolism, expressed in reciprocal days; g denotes grazing rate by zooplankton, expressed in reciprocal days; l' denotes loss rate of zooplankton, expressed in reciprocal days; and γ denotes zooplankton assimilation.

Stressing the significance of the phytoplankton, the vertical phytoplankton model (z -) follows the following mathematical form:

$$\frac{\partial P}{\partial t} - \frac{\partial}{\partial z} \left(E_z \frac{\partial P}{\partial z} \right) + \frac{\partial}{\partial z} (u_z + u_s) P = (\mu - l) P \quad (3)$$

The vertical model study is available to grasp the features of the phytoplankton (Evans and Parslow, 1985; Franks, 1997, 2002; Riley, Stommel, and Bumpus, 1949; Schnoor and Di Toro,

1980; Taylor and Ferrari, 2011; Wong, Lee, and Hodgkiss, 2007). An asymptotic solution $P(z, t) = f(z)e^{kt}$ of Equation (3) is provided by Di Toro (1974). The form of $f(z)$ is written as

$$f(z) = Ke^{az} (a \sin \sqrt{\lambda} z + \sqrt{\lambda} \cos \sqrt{\lambda} z) \quad (4)$$

$$a = \frac{u_z + u_s}{2E_z} \quad (5)$$

$$\lambda = [\mu - (k + l)]/E_z - (u_z + u_s)^2/4E_z^2 \quad (6)$$

where K is a constant defined by the initial condition and k indicates the net phytoplankton growth rate with respect to time interval, estimated as a function of $k = \ln[P(z, t_2)/P(z, t_1)]/(t_2 - t_1)$ (Behrenfeld, 2010; Schnoor and Di Toro, 1980). Here, k is a comprehensive coefficient caused by phytoplankton growth, mortality, respiration, sinking and predation. When the condition of $k = 0$ is satisfied, there is no net growth or loss. Equation (3) is confined within the euphotic zone ($z \leq Z_e$), with sufficient light intensity penetrating the water column. The water column is divided into three layers: an air-water surface layer ($z = 0$), a euphotic layer ($0 < z \leq Z_e$), and a noneuphotic layer ($Z_e < z \leq H$, where H is the total water depth). The noneuphotic layer contains available nutrients but few living species. Thus, the euphotic layer distinguishes the dominated activity of growth or death (Aarup, 2002; Lee *et al.*, 2007; Margalef, 1978).

To explore the solution of the phytoplankton model, the transfer functions should be explored: k , μ , l , u_z , u_s , and E_z . The functions l and u_s are referred to as constants, with $l = 0.05$ after Wei *et al.* (2004); the order of u_s is 10^{-6} after Blauw *et al.* (2009) and Skogen *et al.* (1995). Estimates of the vertical turbulent diffusivity and the phytoplankton growth rate are equally significant in the model.

The vertical mixing process is performed with the Delft3D-flow model, which has been validated in this area (He *et al.*, 2015). The graphical comparisons of water level between model results and observations are shown in Figure 2 (Dafeng station and Yangkou station), from 6 September 2006 to 14 September 2006.

The commonly used estimate of the specific phytoplankton growth rate is as a function of temperature, light intensity, salinity, and nutrients, separately or comprehensively (Eppley, 1972; Geider, MacIntyre, and Kana, 1998; Ornlöf, 2011; Lumsden, and Pinckney, 2004; Smith, 1980; Sofia and Angel, 2011). In this case, the estimate of the growth rate is intended to integrate the temperature function into the light curve.

Skill Assessment

The vertical phytoplankton model is applied to obtain the properties of phytoplankton biomass. Before the application of the model, the reliability of the model must be tested. Skill assessment measures the difference between model results and observations. The root-mean-square error (RMSE) provides a reliable comparison.

In principle, the form of RMSE is defined as follows:

$$\text{RMSE} = \left(\frac{1}{N} \sum_{i=1}^N \Delta^2 \right)^{\frac{1}{2}} \quad (7)$$

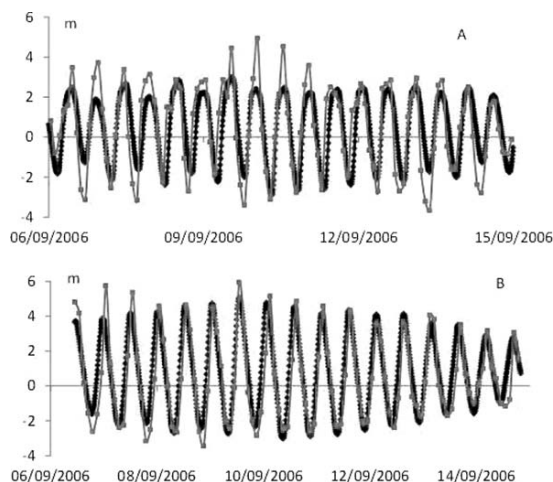


Figure 2. Graphical comparisons of water level between model results (smooth line) and observations (markers) at (A) Dafeng station and (B) Yangkou station in the Jiangsu coastal zone. Most of the model results are consistent with observations.

The use of Δ is defined as

$$\Delta = P_m - P_d \quad (8)$$

where P_m denotes the modeled phytoplankton biomass and P_d denotes the monitored data.

The bias provides a measure of the mean values, defined as follows:

$$\text{Bias} = \bar{P}_m - \bar{P}_d \quad (9)$$

If $\text{Bias} < 0$, P_m is underestimating P_d ; if $\text{Bias} > 0$, P_m is overestimating P_d . The unbiased root-mean-square error (RMSE') is defined as

$$\text{RMSE}'^2 = \text{RMSE}^2 - \text{Bias}^2 \quad (10)$$

with normalized bias (Bias*) by standard deviation (σ_d) of the monitored data

$$\text{Bias}^* = \frac{\text{Bias}}{\sigma_d} \quad (11)$$

and the normalized unbiased root-mean-square error (RMSE'*) defined as follows:

$$\text{RMSE}'^* = \frac{\text{RMSE}'}{P_{d \max} - P_{d \min}} \quad (12)$$

In Equations (9)–(12), \bar{P}_m and \bar{P}_d indicate the mean value of the model output and the monitored data, respectively, and $P_{d \max}$ and $P_{d \min}$ denote the maximum and minimum value of the monitored data, respectively. If the values of Bias* and RMSE'* are out of the range $[-1, 1]$, the results of the model are less reliable.

RESULTS

This research intends to investigate the characteristics of phytoplankton dynamics in the coastal waters of Jiangsu.

Table 1. Statistical analysis of the monitored samples in 2006 at four stations along the Jiangsu coast.

	Lianyungang	Dafeng	Yangkou	Yangtze River Estuary, North Branch
<i>Chla</i> (g m^{-3})				
Mean	3.10	3.91	3.68	5.50
SD	1.03	0.46	1.20	5.29
Min	0.63	3.30	2.45	3.24
Max	5.64	5.20	7.79	25.71
<i>P</i> (g m^{-3})				
Mean	0.54	0.37	0.34	0.38
SD	0.45	0.02	0.04	0.06
Min	0.11	0.33	0.28	0.33
Max	2.63	0.41	0.45	0.58
K_d (day^{-1})				
Mean	0.23	0.27	0.26	0.41
SD	0.06	0.03	0.08	0.48
Min	0.09	0.24	0.19	0.23
Max	0.38	0.35	0.53	2.25
<i>I</i> (Einstein $\text{m}^{-2} \text{day}^{-1}$)				
Mean	30.85	30.06	30.41	30.94
SD	10.99	11.31	11.84	12.12
Min	10.72	10.78	6.85	7.11
Max	50.08	49.88	54.39	55.40
<i>Ze</i> (m)				
Mean	17.34	7.44	7.49	6.11
SD	7.96	2.89	2.73	2.23
Min	5.61	3.17	3.46	3.00
Max	39.51	15.61	14.10	11.69
<i>T</i> ($^{\circ}\text{C}$)				
Mean	15.1	16.5	17.0	17.3
SD	8.1	8.0	7.8	7.8
Min	4.0	5.3	6.3	6.3
Max	26.2	28.4	28.3	28.6

SD = standard deviation.

Concern is focused on the descriptions of the vertical mixing rate and the growth rate among all transfer functions. The vertical model study is able to give insight into phytoplankton dynamics.

Statistical Analysis of the Monitored Variables

The statistical analysis of the monitor samples is displayed in Table 1. The annual variations of two seasonal variables, light intensity and water temperature, show a small difference at four stations. In another words, these two variables can be set as domain parameters. An extreme value of chlorophyll *a* (25.71 mg m^{-3}) appeared on 4 August at the north branch of the Yangtze River estuary, while the maximum phytoplankton biomass (2.63 g m^{-3}) appeared on 30 April at Lianyungang station. The researchers have accepted that chlorophyll *a* is an important measure of phytoplankton biomass (Boyer *et al.*, 2009; Niu *et al.*, 2015a, b, c; Ramirez *et al.*, 2005; Scharler and Baird, 2003). Significant correlations ($R^2 = 0.55 - 0.81$) are established between phytoplankton biomass and chlorophyll *a* in this case, described as $P = Ae^{B \times Chla}$ ($P = 0.1166e^{0.4291 \times Chla}$ and $R^2 = 0.5458$ at Lianyungang station, $P = 0.2238e^{0.1193 \times Chla}$ and $R^2 = 0.6047$ at Dafeng station, $P = 0.2527e^{0.0768 \times Chla}$ and $R^2 = 0.8139$ at Yangkou station, and $P = 0.3268e^{0.0241 \times Chla}$ and $R^2 = 0.7154$ at the north branch of the Yangtze River estuary. Accordingly, the coefficients of *A* and *B* follow a nonlinear function ($B = 2.2547e^{-13.61 \times A}$ and $R^2 = 0.9933$).

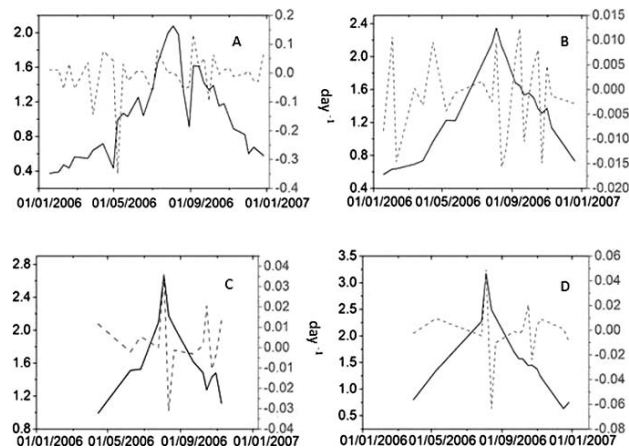


Figure 3. Time series variations of the specific growth rate (smooth line) and the net growth rate (dash line) at four stations along the Jiangsu coastal zone—(A) Lianyungang, (B) Dafeng, (C) Yangkou, and (D) the north branch of the Yangtze River estuary—expressed in reciprocal days. The specific growth rate is estimated from the combined effects of temperature and light intensity, while the net growth rate is derived from the increase of phytoplankton biomass with respect to time interval (8 d or biweekly). The specific growth rate varies with a similar trend of light intensity and temperature, showing higher values on summer days and lower ones in winter.

Another important variable of euphotic depth Z_e ranges from 5.61 to 39.51 m at Lianyungang station, is higher than that at other three stations. Within the layer of Z_e , sufficient light intensity exists to support phytoplankton growth. Light is one of the limiting factors for phytoplankton, especially in winter. Light attenuation coefficient K_d has a close link with Z_e , which can be explained by a function of $I_z = I_0 e^{-K_d z}$ (I_z indicates the incident light intensity at water depth z , expressed in Einstein reciprocal square meters per day, and I_0 indicates available light intensity at the surface layer, expressed in Einstein reciprocal square meters per day) (Devlin *et al.*, 2008; Huisman, van Oostveen, and Weissing, 1999; Sverdrup, 1953). This function has been validated by observations in the Jiangsu coastal zone ($y = 900.96e^{1.333x}$ and $R^2 = 0.9307$, in which y indicates incident light intensity, expressed in micromole photons in square meters per second, and x indicates water depth, expressed in meters), and the data sources are after Liu *et al.* (2012). By a regression analysis, phytoplankton biomass is significantly correlated with the variables of T , K_d , and Z_e ($|r| > 0.6$, $p < 0.01$).

Parameter Estimation

In Figure 3, the specific growth rate shows a seasonal variation, fluctuating with light intensity and temperature. The patterns of the specific growth rate at four stations are similar. The values continually increase in winter, peak on summer days, and then gradually decrease until winter. At Lianyungang station, an abnormal situation happens: the specific growth rate decreases sharply after the maximum value (Figure 3A). The abnormal process is probably caused by the variation of light intensity, reducing quickly from 34 to 20 Einstein $m^{-2} day^{-1}$ during that period.

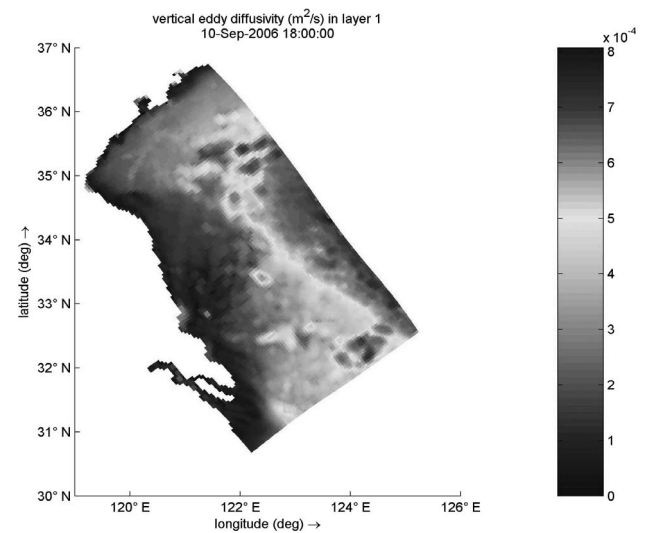


Figure 4. Estimate of the vertical turbulent diffusivity with the Delft3D model, expressed in square meters per second.

In this case, the maximum specific growth rate of $3.17 day^{-1}$ appeared on 4 August at the north branch of the Yangtze River estuary (Figure 3D). The relative temperature and light intensity are all very high— $28.6^{\circ}C$ and 52.89 Einstein $m^{-2} day^{-1}$, respectively. The following maximum value of $2.67 day^{-1}$ appeared at Yangkou station (Figure 3C), with a high temperature of $28.3^{\circ}C$ and a light intensity of 54.39 Einstein $m^{-2} day^{-1}$.

Compared with the variation of the specific growth rate, the net growth rate presents a different pattern in both spatial and temporal dimensions. The positive values state that the phytoplankton production is higher than the loss. Furthermore, bloom events may be triggered when a rapid increase of the net growth rate happens, like on 4 August both at Yangkou station and the north branch of the Yangtze River estuary (Figures 3C and D).

Although the phytoplankton has large growth potential ($\mu = 0.37$ – 2.08 , 0.55 – 2.34 , 0.67 – 2.67 , and 0.63 – $3.17 day^{-1}$ at Lianyungang station, Dafeng station, Yangkou station, and the north branch of the Yangtze River estuary, respectively), the net growth rate varied within ± 0.1 , ± 0.015 , ± 0.03 , and $\pm 0.06 day^{-1}$ over the 8-day interval at the four stations. When the values of k fluctuate around zero, there is no obvious net increase or loss of production.

The estimate of the vertical turbulent diffusivity (10 September) is displayed in Figure 4. The vertical mixing process affects the distributions of phytoplankton biomass, driven by the effects of tidal currents and wind stress. The order of E_z is from 10^{-4} to 10^{-3} in the Jiangsu coastal waters. The annual average estimate of the vertical turbulent diffusivity is $8.09 \pm 3.74 cm^2 s^{-1}$ ($8.07 \pm 3.64 cm^2 s^{-1}$ at Lianyungang station, $7.21 \pm 2.70 cm^2 s^{-1}$ at Dafeng station, $7.26 \pm 3.96 cm^2 s^{-1}$ at Yangkou station, and $10.3 \pm 4.13 cm^2 s^{-1}$ at the north branch of the Yangtze River estuary).

Table 2. Skill assessment results of the vertical phytoplankton model over 2006.

Results by Location (g m^{-3})	\bar{P}_d	\bar{P}_m	σ_d	Bias	Bias*	RMSE	RMSE'	RMSE'*
Lianyungang	0.54	0.48	0.45	-0.06	-0.14	0.59	0.59	0.23
Dafeng	0.37	0.37	0.02	0.00	0.17	0.09	0.09	1.06
Yangkou	0.34	0.31	0.03	-0.03	-0.88	0.07	0.06	0.38
Yangtze River estuary	0.38	0.34	0.07	-0.03	-0.51	0.09	0.08	0.32

Validation of the Vertical Phytoplankton Model

The skill assessment results of the vertical phytoplankton model are shown in Table 2. Figure 5 plots the graphical comparisons between the monitored phytoplankton biomass and the model output. At Lianyungang station, the monitored phytoplankton biomass varied around $0.54 \pm 0.45 \text{ g m}^{-3}$, while the modeled phytoplankton biomass varied around $0.48 \pm 0.55 \text{ g m}^{-3}$. At Dafeng station, the monitored data varied around $0.37 \pm 0.02 \text{ g m}^{-3}$, while the modeled data varied around $0.37 \pm 0.10 \text{ g m}^{-3}$. At Yangkou station, the monitored phytoplankton biomass varied around $0.34 \pm 0.03 \text{ g m}^{-3}$, while the modeled phytoplankton biomass varied around $0.31 \pm 0.07 \text{ g m}^{-3}$. At the north branch of the Yangtze River estuary, the monitored phytoplankton biomass varied around $0.38 \pm 0.07 \text{ g m}^{-3}$, while the modeled phytoplankton biomass varied around $0.34 \pm 0.11 \text{ g m}^{-3}$. The index of RMSE denotes the difference between the model output and the monitored data. The modeled phytoplankton biomass underestimates the monitored data (Bias < 0) at Lianyungang, Yangkou, and the north branch of the Yangtze River estuary, while the modeled values overestimate the monitored data at Dafeng station (Bias > 0). The Bias* and the RMSE' are used to characterize the skill assessment, with 90% inside the range of [-1, 1]. It is concluded that the vertical phytoplankton model is able to reproduce reliable predictions of phytoplankton biomass in this study.

Model Output

In this section, the model output of phytoplankton biomass is discussed in the case study of the Jiangsu coastal waters. For the vertical dimension, the water column is subdivided into several water layers: 2, 5, 10, and 20 m. The statistics of phytoplankton biomass are displayed in Table 3. In spring, the phytoplankton biomass is higher at Lianyungang station than

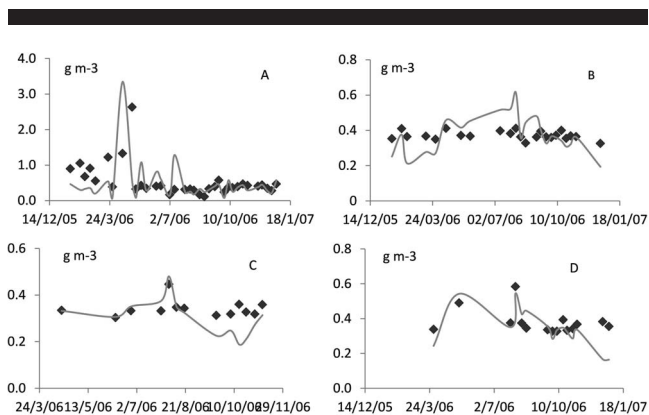


Figure 5. Graphical comparisons of the monitored phytoplankton biomass (scatters) and the model output (smooth line) over 2006 in the Jiangsu coastal zone, expressed in grams per cubic meter.

that at the other three stations. A decrease of phytoplankton biomass corresponds to deeper water, excluding the case of Yangkou station.

For the water depth of 2 m at Lianyungang station, the minimum value 0.01 g m^{-3} appeared on 30 April, and the maximum value 3.07 g m^{-3} appeared on 14 April. Higher values appeared in spring and autumn. The average value was 0.36 g m^{-3} , and the standard deviation was 0.51 g m^{-3} . At Dafeng station, the annual fluctuation was relatively steady, with a mean value of 0.28 g m^{-3} and a standard deviation of 0.15 g m^{-3} . The minimum value 0.03 g m^{-3} appeared on 10 February, and the value maximum 0.57 g m^{-3} appeared on 26 July. At Yangkou station, the phytoplankton biomass varied within a range of 0.01 to 0.28 g m^{-3} . The minimum value appeared on 19 August, and the maximum value appeared on 4 August. At the north branch of the Yangtze River estuary, the phytoplankton biomass varied around $0.21 \pm 0.16 \text{ g m}^{-3}$.

Similar to the water depth of 2 m, the phytoplankton biomass for the water depth of 5 m varied, with a big difference at Lianyungang station, ranging from 0.02 to 3.34 g m^{-3} . At Dafeng station, the phytoplankton biomass varied within a range of 0.03 to 0.57 g m^{-3} , with a mean value of 0.27 g m^{-3} and a standard deviation of 0.14 g m^{-3} . At Yangkou station and the north branch of the Yangtze River estuary, the values of phytoplankton biomass were relatively smaller, varying within the ranges of 0.02 to 0.35 and 0.002 to 0.51 g m^{-3} , respectively.

For the water depth of 10 m at Lianyungang station, the phytoplankton biomass varied within a range of 0.005 to 2.95 g

Table 3. Statistics of phytoplankton biomass for the different water layers in the Jiangsu coastal waters.

Statistics by Location (g m^{-3})	2 m	5 m	10 m	20 m
Lianyungang				
Min	0.014	0.024	0.006	0.001
Max	3.373	4.138	4.350	3.638
Mean	0.366	0.357	0.448	0.396
SD	0.558	0.662	0.736	0.608
Dafeng				
Min	0.029	0.030	0.027	0.007
Max	0.576	0.572	0.559	0.571
Mean	0.283	0.276	0.261	0.263
SD	0.148	0.143	0.127	0.154
Yangkou				
Min	0.016	0.023	0.001	0.012
Max	0.282	0.346	0.343	0.502
Mean	0.165	0.191	0.150	0.226
SD	0.085	0.100	0.110	0.146
Yangtze estuary				
Min	0.013	0.003	0.052	0.002
Max	0.551	0.513	0.722	0.470
Mean	0.207	0.232	0.219	0.278
SD	0.163	0.145	0.179	0.132

SD = standard deviation.

Table 4. Statistical analysis of the depth-averaged phytoplankton biomass in the Jiangsu coastal waters.

Results by Location (g m^{-3})	Statistics	Bootstrap*			
		Bias	Std. Error	95% Confidence Interval	
				Lower	Upper
Lianyungang					
Mean	0.496	-0.007	0.194	0.232	0.911
SD	0.712	-0.132	0.330	0.110	1.102
Skewness	3.091	-1.114	1.031	-0.090	3.470
Dafeng					
Mean	0.279	-0.001	0.025	0.230	0.331
SD	0.082	-0.005	0.014	0.060	0.118
Skewness	0.054	-0.088	0.466	-0.992	0.998
Yangkou					
Mean	0.198	0.001	0.015	0.169	0.229
SD	0.058	-0.004	0.010	0.035	0.075
Skewness	0.639	-0.190	0.563	-0.747	1.643
Yangtze River estuary					
Mean	0.280	0.001	0.027	0.236	0.336
SD	0.097	-0.009	0.029	0.037	0.140
Skewness	1.866	-0.479	0.690	0.071	2.776

* Unless otherwise noted, bootstrap results are based on 500 bootstrap samples. The objects of the bootstrap method are the estimates of mean value, standard deviation (SD), and skewness.

Std. error = standard error.

m^{-3} , with a mean value of 0.41 g m^{-3} and a standard deviation of 0.53 g m^{-3} . The minimum appeared on 6 May, and the maximum appeared on the same day as other water depths. Higher values appeared in the months of April, May, and July. The phytoplankton biomass fluctuated with 0.26 ± 0.13 , 0.15 ± 0.11 , and $0.22 \pm 0.18 \text{ g m}^{-3}$ at Dafeng station, Yangkou station, and the north branch of the Yangtze River estuary, respectively.

For the water depth of 20 m at Lianyungang station, the minimum value appeared on 1 July. The values became smaller with deeper water. At Dafeng station, the phytoplankton biomass varied within a range of 0.007 to 0.57 g m^{-3} , with a mean value of 0.26 g m^{-3} and a standard deviation of 0.15 g m^{-3} . At Yangkou station, the values became higher with deeper water. The phytoplankton biomass varied from 0.01 to 0.50 g m^{-3} , with a mean value of 0.22 g m^{-3} and a standard deviation of 0.14 g m^{-3} . At the north branch of the Yangtze River estuary, the phytoplankton biomass ranged from 0.002 to 0.47 g m^{-3} , with a mean value of 0.27 g m^{-3} and a standard deviation of 0.13 g m^{-3} .

Particular attention is paid to the depth-averaged phytoplankton biomass in the Jiangsu coastal waters, shown in Table 4. At Lianyungang station, the depth-averaged phytoplankton biomass varied within a range of 0.05 to 2.76 g m^{-3} , with a mean value of 0.49 g m^{-3} and a standard deviation of 0.71 g m^{-3} . At Dafeng station, the depth-averaged phytoplankton biomass varied around $0.28 \pm 0.08 \text{ g m}^{-3}$, with results of 0.20 ± 0.06 and $0.28 \pm 0.09 \text{ g m}^{-3}$ at Yangkou station and the north branch of the Yangtze River estuary, respectively.

DISCUSSION

To get a practical solution for the vertical phytoplankton model, the present study simplifies the real problems. A simplification of the model is accompanied with uncertainty.

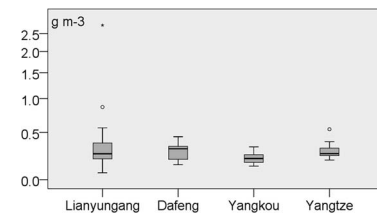


Figure 6. Boxplot of the depth-averaged phytoplankton biomass in the Jiangsu coastal waters, in which the middle black line indicates the median, the shaded region stating the middle 50%. The lines extending out of the shaded region are the top and bottom 25% of the data, and the horizontal lines at the top and bottom of the boxplot are the minimum and maximum values (nonextreme), respectively. One case is classified as the extreme value at Lianyungang station (2.76 g m^{-3}).

The bootstrap method is used to give insight into the 95% confidence interval of the estimate with a characterization of uncertainty analysis, shown in Table 4. At Lianyungang station, the mean value varied from 0.23 to 0.91 g m^{-3} within the 95% confidence interval, with a bias of -0.007 g m^{-3} . At Dafeng station, the mean value varied from 0.23 to 0.33 g m^{-3} within the 95% confidence interval, with a bias of -0.001 g m^{-3} . At Yangkou station, the mean value varied from 0.17 to 0.23 g m^{-3} within the 95% confidence interval, with a bias of 0.001 g m^{-3} and a standard error of 0.015 g m^{-3} . At the north branch of the Yangtze River estuary, the mean value varied from 0.23 to 0.33 g m^{-3} within the 95% confidence interval.

From the index of skewness, the distributions of the depth-averaged phytoplankton biomass have a long right tail at Lianyungang station (3.091) and at the north branch of the Yangtze River estuary (1.866), deviating largely from the center. The potential extreme values of phytoplankton biomass may appear at these two stations resulting from the boxplot analysis displayed in Figure 6. The open dots indicate the higher values of phytoplankton biomass (nonextreme), and the black star indicates the extreme value. The probability distribution model of Weibull is explored to perform the good-of-fit test at Lianyungang station and at the north branch of the Yangtze River estuary, presented as Figures 7A and D, respectively. The values of skewness are relatively smaller at Dafeng station (0.054) and Yangkou station (0.639), revealing that the symmetric distribution can fit with the data. Figures 7B and C display the good-of-fit test of normal distribution at these two stations, respectively.

CONCLUSIONS

The role of the vertical mixing rate on the phytoplankton is significant, controlling the vertical distributions of phytoplankton biomass and affecting light and nutrient availability. The vertical process is performed with the Delft3D model in this study. To what extent can the vertical phytoplankton model be trusted in this case? This question is processed with the validation of the model: skill assessment (Table 2) and graphical comparisons (Figure 5). The phytoplankton biomass is significantly correlated with the variables of temperature, light attenuation coefficient, and euphotic depth. Higher

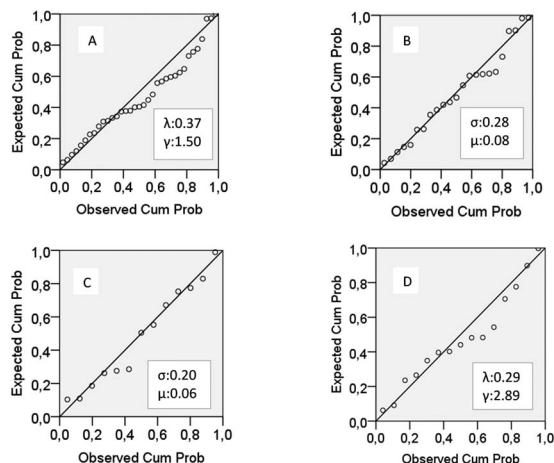


Figure 7. Good-of-fit test using the probability distribution models of Weibull and normal, determined by the depth-averaged phytoplankton biomass over 2006 in the Jiangsu coastal waters. Here, the x-axis indicates the cumulative probability of the model output, the y-axis indicates the cumulative probability of the prediction with random effects, λ is the shape parameter for the Weibull distribution, γ is the scale parameter for the Weibull distribution, μ is the mean value for the normal distribution, and σ is the standard deviation for the normal distribution. (A) Lianyungang station (Weibull distribution), (B) Dafeng station (normal distribution), (C) Yangkou station (normal distribution), and (D) the north branch of the Yangtze River estuary (Weibull distribution).

phytoplankton biomass appears in spring but is lower in winter because of the strong turbulence and light limitation.

The findings of this study contribute to the understanding of ecosystem processes and dynamics. Information on nutrients, grazing, and loss rate will help in increasing the sensitivity of this modeling approach. Future work will further research these issues.

ACKNOWLEDGMENTS

This study is supported by the China Scholarship Council. The authors thank NASA, the Hydrological Bureau of the Yangtze Water Conservancy Committee, and the State Oceanic Administration of the People's Republic of China for providing the data used in this study. The authors also thank the anonymous reviewers.

LITERATURE CITED

Aarup, T., 2002. Transparency of the North Sea and Baltic Sea—A Secchi depth data mining study. *Oceanologia*, 44(3), 323–327.

Behrenfeld, M.J., 2010. Abandoning Sverdrup's critical depth hypothesis on phytoplankton blooms. *Ecology*, 91(4), 977–989.

Blauw, A.; Los, F.J.; Bokhorst, M., and Erftemeijer, L.A., 2009. GEM: A generic ecological model for estuaries and coastal waters. *Hydrobiologia*, 618, 175–198.

Boyer, J.N.; Kelble, C.R.; Ortner, P.B., and Rudnick, D.T., 2009. Phytoplankton bloom status: Chlorophyll *a* biomass as an indicator of water quality condition in the southern estuaries of Florida, USA. *Ecological Indicators*, 9(6), S56–S67.

Cloern, J.E., 1987. Turbidity as a control on phytoplankton biomass and productivity in estuaries. *Continental Shelf Research*, 7, 1367–1381.

Cloern, J.E., 1996. Phytoplankton bloom dynamics in coastal ecosystems: A review with some general lessons from sustained

investigation of San Francisco Bay, California. *Reviews of Geophysics*, 34(2), 127–168.

Cloern, J.E.; Foster, S.Q., and Kleckner, A.E., 2014. Phytoplankton primary production in the world's estuarine-coastal ecosystems. *Biogeosciences*, 11(9), 2477–2501.

Devlin, M.J.; Bary, J.; Mills, D.K.; Gowen, R.J.; Foden, J.; Sivyer, D., and Tett, P., 2008. Relationships between suspended particulate material, light attenuation and Secchi depth in UK marine waters. *Estuarine, Coastal and Shelf Science*, 79(3), 429–439.

Di Toro, D.M., 1974. Vertical interactions in phytoplankton populations—An asymptotic eigenvalue analysis (IFYGL). *Proceedings of the 17th Conference on Great Lakes Research*, pp. 17–27.

Edelvang, K.; Kaas, H.; Erichsen, A.C.; Alvarez-Berasteguil, D.; Bundgaard, K., and Jrgensen, P.V., 2005. Numerical modelling of phytoplankton biomass in coastal waters. *Marine Systems*, 57(1–2), 13–29.

Eilers, P.H.C. and Peeters, J.C.H., 1988. A model for the relationship between light intensity and the rate of photosynthesis in phytoplankton. *Ecological Modelling*, 42, 199–215.

Eppley, R.W., 1972. Temperature and phytoplankton growth in the sea. *Fishery Bulletin*, 70(4), 1063–1085.

Evans, G.T. and Parslow, J.S., 1985. A model of annual plankton cycles. *Biological Oceanography*, 3(3), 327–347.

Ferris, J.M. and Christian, R., 1991. Aquatic primary production in relation to microalgal responses to changing light: A review. *Aquatic Sciences*, 53(2), 187–217.

Franks, P.J.S., 1997. Models of harmful algal blooms. *Limnology and Oceanography*, 42(5), 1273–1282.

Franks, P.J.S., 2002. NPZ models of plankton dynamics: Their construction, coupling to physics, and application. *Journal of Oceanography*, 58, 379–387.

Fu, M.Z.; Wang, Z.L.; Li, Y.; Li, R.X.; Sun, P.; Wei, X.H.; Lin X.Z., and Guo, J.S., 2009. Phytoplankton biomass size structure and its regulation in the southern Yellow Sea (China): Seasonal variability. *Continental Shelf Research*, 29(18), 2187–2194.

Geider, R.J.; MacIntyre, H.L., and Kana, T.M., 1998. A dynamic regulatory model of phytoplankton acclimation to light, nutrients, and temperature. *Limnology and Oceanography*, 43(4), 679–694.

Godrijan, J.; Daniela, M.; Igor, T.; Robert, P., and Martin, P., 2013. Seasonal phytoplankton dynamics in the coastal waters of north-eastern Adriatic Sea. *Journal of Sea Research*, 77, 32–44.

He, X.; Wang, Y.P.; Zhu, Q.; Zhang, Y.; Zhang, D.; Zhang, J.; Yang, Y., and Gao, J., 2015. Simulation of sedimentary dynamics in a small-scale estuary: The role of human activities. *Environmental Earth Science*, 74(1), 869–878. doi:10.1007/s12665-015-4100-9

Huisman, J.; van Oostveen, P., and Weissing, F.J., 1999. Critical depth and critical turbulence: Two different mechanisms for the development of phytoplankton blooms. *Limnology and Oceanography*, 44(1), 1781–1787.

Lee, Z.P.; Weidemann, A.; Kindle, J.; Arnone, R.; Carder, K.L., and Davis, C., 2007. Euphotic zone depth: Its derivation and implication to ocean-color remote sensing. *Journal of Geophysical Research*, 112, 1–11.

Lionard, M.; Muylaert, K.; van Gansbeke, D., and Vyverman, W., 2005. Influence of changes in salinity and light intensity on growth of phytoplankton communities from the Scheldt river and estuary (Belgium/the Netherlands). *Hydrobiologia*, 540(1–3), 105–115.

Liu, F.; Pang, S.J.; Zhao, X.B., and Hu, C.M., 2012. Quantitative, molecular and growth analyses of *Ulva* microscopic propagules in the coastal sediment of Jiangsu province where green tides initially occurred. *Marine Environmental Research*, 74, 56–63.

Margalef, R., 1978. Life-form of phytoplankton as survival alternatives in an unstable environment. *Oceanologica Acta*, 1(4), 493–509.

Murray, A.G. and Parslow, J.S., 1999. The analysis of alternative formulations in a simple model of a coastal ecosystem. *Ecological Modelling*, 119(2–3), 149–166.

NASA (National Aeronautics and Space Administration), 2015. *OceanColor Web*. <http://oceancolor.gsfc.nasa.gov/cms/>.

Niu, L.; Van Gelder, P.H.A.J.M.; Guan, Y.; Zhang, C., and Vrijling, J.K., 2015a. Probabilistic analysis of phytoplankton biomass at the

- Frisian Inlet (NL). *Estuarine, Coastal and Shelf Science*, 155, 29–37.
- Niu, L.; Van Gelder, P.H.A.J.M.; Guan, Y., and Vrijling, J.K., 2015b. Uncertainty analysis and modelling of phytoplankton dynamics in coastal waters. *Environment Protection and Sustainable Development*, 1(4), 193–202.
- Niu, L.; Van Gelder, P.H.A.J.M.; Zhang, C.; Yiqing, G., and Vrijling, J.K., 2015c. Statistical analysis of phytoplankton biomass in coastal waters: Case study of the Wadden Sea near Lauwersoog (the Netherlands) from 2000 through 2009. *Ecological Informatics*, 30, 12–19.
- Ornoldsdottir, E.B.; Lumsden, S.E., and Pinckney, J.L., 2004. Nutrient pulsing as a regulator of phytoplankton abundance and community composition in Galveston Bay, Texas. *Journal of Experimental Marine Biology and Ecology*, 303(2), 197–220.
- Pedersen, M.F. and Borum, J., 1996. Nutrient control of algal growth in estuarine waters: Nutrient limitation and the importance of nitrogen requirements and nitrogen storage among phytoplankton and species of macroalgae. *Marine Ecology Progress Series*, 142, 261–272.
- Ramirez, T.; Cortes, D.; Mercado, J.M.; Vargas-Yanez, M.; Sebastian, M., and Liger, E., 2005. Seasonal dynamics of inorganic nutrients and phytoplankton biomass in the NW Alboran Sea. *Estuarine, Coastal and Shelf Science*, 65(4), 654–670.
- Riley, G.A.; Stommel, H., and Bumpus, D.F., 1949. Quantitative ecology of the plankton of the western North Atlantic. *Bulletin of the Bingham Oceanographic Collection, Yale University*, 12, 1–169.
- Scharler, U.M. and Baird, D., 2003. The influence of catchment management on salinity, nutrient stoichiometry and phytoplankton biomass of eastern cape estuaries, South Africa. *Estuarine, Coastal and Shelf Science*, 56(3–4), 735–748.
- Schmidt, I., 1999. The importance of phytoplankton biomass as an ecosystem parameter in shallow bays of the Baltic: I. Relationships between biomass and system characteristics. *Limnologica*, 29, 301–307.
- Schnoor, J.L. and Di Toro, D.M., 1980. Differential phytoplankton sinking and growth rates: An eigenvalue analysis. *Ecological Modelling*, 9, 233–245.
- Serra, T.; Vidal, J.; Casamitjana, X.; Soler, M., and Colomer, J., 2007. The role of surface vertical mixing in phytoplankton distribution in a stratified reservoir. *Limnology and Oceanography*, 52(2), 620–634.
- Sharples, J., 2007. Potential impacts of the spring–neap tidal cycle on shelf sea primary production. *Plankton Research*, 30(2), 183–197.
- Sharples, J.; Moore, C.M.; Rippeth, T.P.; Holligan, P.M.; Hydes, D.J., and Fisher, N.R., 2001. Phytoplankton distribution and survival in the thermocline. *Limnology and Oceanography*, 46(3), 486–496.
- Skogen, M.D.; Svendsen, E.; Berntsen, J.; Aksnes, D., and Ulvestad, K.B., 1995. Modelling the primary production in the North Sea using a coupled three-dimensional physical–chemical–biological ocean model. *Estuarine, Coastal and Shelf Science*, 41(5), 545–565.
- Smith, R.A., 1980. The theoretical basis for estimating phytoplankton production and specific growth rate from chlorophyll, light and temperature data. *Ecological Modelling*, 10, 243–264.
- Sofia, S. and Angel, L.U., 2011. Comment: Temperature, nutrients, and the size-scaling of phytoplankton growth in the sea. *Limnology and Oceanography*, 56(5), 1952–1955.
- Sverdrup, H.U., 1953. On conditions for the vernal blooming of phytoplankton. *Journal du Conseil International pour l'Exploration de la Mer*, 18, 287–295.
- Taylor, J.R. and Ferrari, R., 2011. Shutdown of turbulent convection as a new criterion for the onset of spring phytoplankton blooms. *Limnology and Oceanography*, 56(6), 2293–2307.
- Wei, H.; Sun, J.; Moll, A., and Zhao, L., 2004. Phytoplankton dynamics in the Bohai sea—Observations and modelling. *Marine Systems*, 44(3–4), 233–251.
- Wild-Allen K.; Lane, A., and Tett, P., 2002. Phytoplankton, sediment and optical observations in Netherlands coastal water in spring. *Journal of Sea Research*, 47(3–4), 303–315.
- Williams, E. and Rhines, P.B., 2010. Physical controls and interannual variability of the Labrador Sea spring phytoplankton bloom in distinct regions. *Deep-Sea Research I*, 57, 541–552.
- Woernle, L.H.; Dijkstra, H.A., and van der Woerd, H.J., 2014. Sensitivity of phytoplankton distributions to vertical mixing along a North Atlantic transect. *Ocean Science*, 10, 993–1011.
- Wong, K.T.M.; Lee, J.H.W., and Hodgkiss, I.J., 2007. A simple model for forecast of coastal algal blooms. *Estuarine, Coastal and Shelf Science*, 74(1–2), 175–196.